Editors' Suggestion

Identification of the New Isotope ^{244}Md

J. L. Pore,[1,*] J. M. Gates,[1] R. Orford,[1] C. M. Campbell,[1] R. M. Clark,[1] H. L. Crawford,[1] N. E. Esker,[2] P. Fallon,[1] J. A. Gooding,[3,1] J. T. Kwarsick,[1] A. O. Macchiavelli,[1] C. Morse,[1] D. Rudolph,[4] A. Såmark-Roth,[4] C. Santamaria,[1] R. S. Shah,[3] and M. A. Stoyer[1,5]

[1]*Nuclear Science Division, Lawrence Berkeley National Laboratory, One Cyclotron Road, Berkeley, California 94720, USA*
[2]*Department of Chemistry, San José State University, One Washington Square, San José, California 95192, USA*
[3]*University of California Berkeley, Berkeley, California 94720, USA*
[4]*Department of Physics, Lund University, SE-22100 Lund, Sweden*
[5]*Lawrence Livermore National Laboratory, 7000 East Avenue, Livermore, California 94550, USA*

(Received 31 January 2020; revised manuscript received 10 April 2020; accepted 12 May 2020; published 23 June 2020; corrected 28 July 2020)

In an experiment performed at Lawrence Berkeley National Laboratory's 88-inch cyclotron, the isotope ^{244}Md was produced in the ^{209}Bi(^{40}Ar, $5n$) reaction. Decay properties of ^{244}Md were measured at the focal plane of the Berkeley Gas-filled Separator, and the mass number assignment of $A = 244$ was confirmed with the apparatus for the identification of nuclide A. The isotope ^{244}Md is reported to have one, possibly two, α-decaying states with α energies of 8.66(2) and 8.31(2) MeV and half-lives of $0.4^{+0.4}_{-0.1}$ and ~6 s, respectively. Additionally, first evidence of the α decay of ^{236}Bk was observed and is reported.

DOI: 10.1103/PhysRevLett.124.252502

Recently, there have been numerous studies to investigate neutron-deficient heavy nuclei that undergo the rare decay mode electron capture-delayed fission (ECDF) [1]. These measurements are important, as they allow access to exotic cases of low-energy fission that are not yet accessible by any other technique. However, data in these regions are scarce, and more detailed measurements need to be made. Isotopes in this region ($Z \sim 100$) are produced in fusion-evaporation reactions and studied with the use of recoil gas-filled separators [2] or velocity filters [3–5]. In such studies, several neighboring isotopes of a given element can be created simultaneously from the different exit channels of a single nuclear reaction. It is not uncommon for neighboring isotopes to have similar decay properties, which can make it a challenge to assign decay properties to a specific isotope.

The recent coupling of FIONA (for the identification of nuclide A) [6] to the Berkeley Gas-filled Separator (BGS) [7] at the Lawrence Berkeley National Laboratory 88-inch cyclotron facility now allows for the separation and identification of individual atoms of heavy elements by their mass number-to-charge-state ratio (A/q). This setup is ideal for measurements to discover and characterize new isotopes, as their decay properties can be observed with high efficiency at the BGS focal plane, in combination with a unique mass-number confirmation with FIONA [8].

In this work, we report on the first identification of the isotope ^{244}Md produced in the ^{209}Bi(^{40}Ar, $5n$)^{244}Md reaction. We understand that during the course of this work a parallel effort to discover ^{244}Md has been ongoing [9]. We present confirmation of the $A = 244$ mass number as well as the observed decay properties of ^{244}Md. This study is part of a campaign of measurements on neutron-deficient Md isotopes performed with the combined BGS and FIONA setup [10].

The experiment was performed at the Lawrence Berkeley National Laboratory's 88-inch cyclotron facility. The BGS and FIONA were tuned and calibrated with ions of ^{247}Md and $^{199-201}$At created in the ^{209}Bi(^{40}Ar, $2n$) and ^{165}Ho(^{40}Ar, 4-6n) reactions, respectively. The purpose was to establish experimental procedures by confirming that we could identify ^{247}Md by its mass number $A = 247$ with FIONA. Then, ions of ^{244}Md and $^{198-199}$At were created in the ^{209}Bi(^{40}Ar, $5n$) and ^{165}Ho(^{40}Ar, 6-7n) reactions, respectively.

A beam of ^{40}Ar^{9+} was produced from enriched-argon gas in the Advanced Electron Cyclotron Resonance ion source [11]. The ions were accelerated to laboratory-frame energies of approximately 200 MeV for production of ^{247}Md and $^{199-201}$At ions and to approximately 220 MeV for the production of ^{244}Md and $^{198-199}$At ions. Sustained beam intensities of 15 eμA of ^{40}Ar^{9+} ions on target were achieved.

The beam was incident on a 4"-diameter target wheel rotating at ~30 Hz, located just upstream of the BGS. The target wheel contained four target segments: three segments of ^{209}Bi with an average thickness of 0.500 mg/cm^2 for the production of Md isotopes and a fourth segment made of ^{165}Ho with an average thickness of 0.365 mg/cm^2 for the production of At isotopes. Each segment was prepared via vapor deposition on 2.1-μm-thick titanium backing foils. Two silicon pin diode detectors were positioned in the target chamber at angles of $\pm 27.2°$ relative to the beam axis to measure Rutherford scattered beam particles, which

 © 2020 American Physical Society

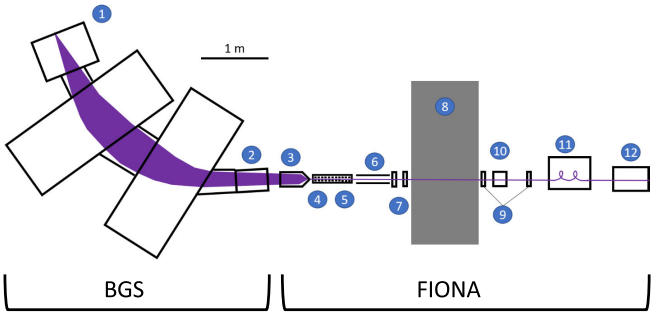

FIG. 1. Schematic of the coupled BGS plus FIONA setup with the labels indicating the positions of (1) BGS, (2) BGS focal-plane detector, (3) gas catcher, (4) RFQ cooler, (5) RFQ trap, (6) acceleration region, (7) focusing element and horizontal and vertical steerers, (8) shielding wall, (9) focusing element and horizontal and vertical steerers, (10) diagnostic DSSD detector, (11) trochoid spectrometer, and (12) FIONA focal-plane detector. The purple shaded area and line represent the trajectory of the ions as they travel through the BGS and FIONA.

allowed for a continuous monitor of the integrated beam intensity, target thickness, and target integrity.

The produced Md and At ions recoiled out of the target and were separated from unreacted beam and nuclear-reaction products in the BGS. A schematic drawing of the coupled BGS plus FIONA setup is presented in Fig. 1. It depicts the trajectory of the ions of interest as they travel through the system. At the BGS focal plane (Fig. 1, label 2), either ions can be implanted into a retractable 32×32 double-sided silicon strip detector (DSSD) for detection of decay properties, or, if the detector is extracted, the ions pass through a 2.1-μm-thick Ti foil entering the FIONA apparatus.

Upon entering FIONA, the Md and At ions were stopped in 10 kPa of ultrapure He gas inside of a radio frequency (rf) gas catcher (Fig. 1, label 3). There they underwent charge-exchange reactions with the gas until they reached an equilibrated distribution of charge states. The distribution of charge states for a particular element is dependent upon its first, second, and third ionization potentials (IPs) relative to that of the He gas as well as any other contaminants that may be present in the system (such as O_2 or N_2). Under the experimental conditions, the At ions [$IP_2 = 17.880(20)$ eV [12]] stop primarily as $1+$ ions, and the Md ions [$IP_2 = 12.4(4)$ eV [13]] stop primarily as $2+$ ions. A direct current (dc) electric field gradient was applied along the gas catcher, causing the stopped ions to drift toward the exit orifice with an average drift time estimated to be ~28 ms, which is based on a reduced ion mobility of 20×10^4 V × s.

After exiting the rf gas catcher, the ions were confined by an rf quadrupole (RFQ) field, while the He gas was differentially pumped to a pressure of ~30 Pa. A dc gradient, applied along the RFQ axis, directed the ions downstream, where they were captured in an RFQ trap, which was configured with an axial dc gradient profile to create a three-dimensional trapping potential (Fig. 1, labels 4 and 5). The RFQ trap contained ~2 Pa of He buffer gas, where collisions of the ions with the gas cool them to several times thermal energies in a volume of 1 mm^3. The cooled ions were trapped for ~25 ms before being ejected. Once ejected, the ions passed through a region containing acceleration electrodes, steering electrodes, and Einzel lenses (Fig. 1, labels 6 and 7) before they entered a low-γ and neutron radiation background area separated from the high-background area by a shielding wall (Fig. 1, label 8).

In the low-background area, the ions were separated by their A/q in a trochoidal spectrometer (Fig. 1, label 11) [6]. The spectrometer utilizes crossed magnetic and electric fields, tuned to force the ions traveling through the spectrometer to take trochoidal trajectories [14–17]. These trajectories are heavily dependent on a particular ion's A/q and are largely independent of its velocity. This results in an A/q-angular separation of ions as they exit the spectrometer due to the difference in the exiting-trochoid phase of ions with different A/q. The A/q dispersion for ions detected at the FIONA focal plane, ~75 cm downstream (Fig. 1, label 12) after they exited the trochoidal spectrometer, is ~20 mm per-percent difference in A/q. The trochoidal spectrometer consists of a relatively small flat-field magnet ($l \times w \times h = 50$ cm $\times$ 50 cm $\times$ 8 cm) with a maximum magnetic field of 1.1 T in the downward (gravity) direction, perpendicular to the beam direction. Inside the magnet vacuum chamber, top- and bottom-striped circuit boards with resistor chains create a uniform electric field perpendicular to both the magnetic field and the velocity vector of the entering ions.

At the FIONA and (optionally) BGS focal planes, ions are implanted, or deposited at FIONA, into 32×32 strip DSSDs that are 1 mm thick with active areas of 60 mm $\times$ 60 mm. Energies for events detected in the DSSDs were calibrated using a source containing ^{239}Pu, ^{241}Am, and ^{244}Cm. The position of a detected event was given by the horizontal and vertical strip number in which the event was detected. The data acquisition was triggered by an event detected in the DSSD with an energy above ~1 MeV.

To optimize the efficiency and A/q resolution of FIONA, ions of $^{198-201}At^{1+}$ were used to tune the ion acceleration, focusing elements, steerers, and trochoidal separator. A typical efficiency from the BGS focal plane through FIONA for detection at the FIONA focal plane is 15%, and the mass-resolving power, with separation of masses at the full-width-at-tenth-maximum level, is $(A/q)/\Delta(A/q) = 250$.

In order to make a mass number identification, to confirm $(A/q)_{new}$, the FIONA system was scaled from the $(A/q)_{cal}$ settings of the At^{1+} ions such that ions of $(A/q)_{new}$ would have the same magnetic rigidity as $(A/q)_{cal}$. The $^{198-201}$At isotopes have been well studied [18–21], so the A of a particular At^{1+} isotope delivered to

the FIONA focal plane can be readily identified from decay properties. For this measurement, the calibration procedure ensures that the $(A/q)_{\mathrm{new}}$ ions took the same trajectory through FIONA as the $(A/q)_{\mathrm{cal}}$ calibration ions, such that they would be detected in the same position in the FIONA focal plane DSSD. To do this, the voltages applied to the RFQ trap ejection electrodes, steering and focusing electrodes, and the electrodes inside the trochoidal spectrometer were scaled by $(A/q)_{\mathrm{cal}}/(A/q)_{\mathrm{new}}$. Additionally, to match the electric rigidity of the ions, the time between releasing the ions from the RFQ trap and the pulsing drift tube in the acceleration region was scaled by $(A/q)_{\mathrm{new}}/(A/q)_{\mathrm{cal}}$. FIONA was recalibrated approximately every 8 h to account for any potential drifts in the system. Examples of this calibration procedure are shown in Ref. [8].

Evaporation residue (EVR)-α-α correlations were searched for in data taken at the 200 MeV beam energy with the BGS focal plane detector inserted. Search conditions were EVR energy $E_{\mathrm{EVR}} = 13$–20 MeV, α_1 energy 8–9 MeV, α_2 energy 7–9 MeV, EVR-α_1 $\Delta t < 10$ s, and α_1-α_2 $\Delta t < 100$ s. Here, α_1 and α_2 refer to the first and second particles observed in the same pixel as the detected EVR, respectively. Additionally, EVR-α_1 Δt and α_1-α_2 Δt are the time differences in detection for each respective pair of particles. At the BGS focal plane, we are not sensitive to EVR-fission events due to high-random rates of events with fissionlike energies. The detection efficiency for EVR-α-α events is 25%. Multiple EVR-α-α correlations were identified with properties consistent with known decay properties of the isotope ^{247}Md, with parent ^{247}Md $E_{\alpha 1} = 8$–9 MeV with half-life $t_{1/2} \sim 1$ s and daughter ^{243}Es $E_{\alpha 2} = 7$–8 MeV with $t_{1/2} \sim 20$ s [22]. These data will be discussed in more detail in a forthcoming publication [10]. To confirm the mass number $A = 247$ of the produced Md isotope, the BGS focal plane DSSD was removed and the Md ions were transmitted to the FIONA focal plane.

FIONA was calibrated using the $^{199-201}$At^{1+} ions. The system was scaled from $(A/q)_{\mathrm{cal}} = 200/1$ to $(A/q)_{\mathrm{new}} = 247/2$ for the delivery of the Md^{2+} ions to the FIONA focal plane. As shown in Fig. 2, the Md^{2+} ions were detected in the same position as the ^{200}At^{1+} ions at the FIONA focal plane. This allows for a mass number confirmation of $A = 247$.

After demonstrating the identification of ^{247}Md with FIONA, the dataset taken with the BGS focal plane detector at the 220 MeV beam energy was searched for EVR-α-α correlations using the same event selection windows stated previously. Time windows were expanded to 30 and 300 s for EVR-α_1 Δt and α_1-α_2 Δt, respectively, to look for longer-lived decays. None were observed with EVR-α_1 $\Delta t > 10$ s. Data were collected for ~35 h. From analysis of the rate of both EVR-like and α-like events observed per pixel, during the run time, 0.1 random EVR-α-α correlations were expected. Overall, six EVR-α-α correlations were identified (including one EVR-α_1-α_2-α_3 event).

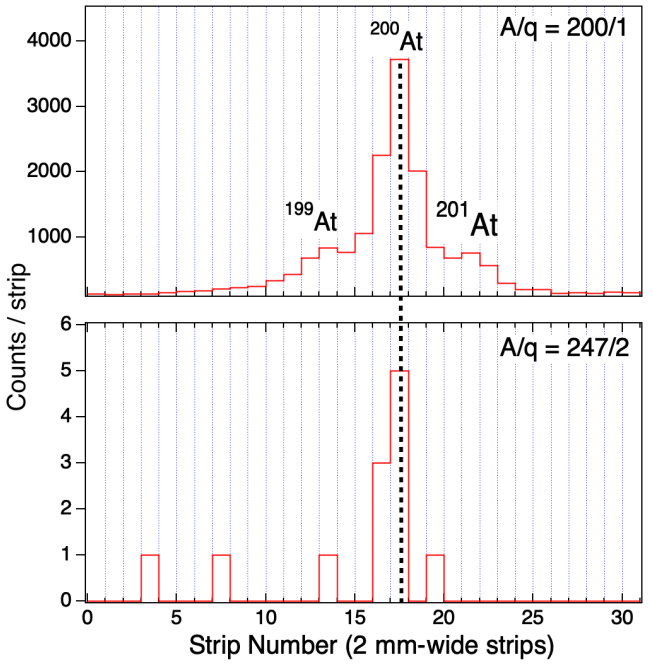

FIG. 2. (Top) Experimental data from an example $^{199-201}$At^{1+} calibration run showing the A/q separation. (Bottom) Location of the detection of Md^{2+} ions after FIONA was scaled from $(A/q)_{\mathrm{cal}} = 200/1$ to $(A/q)_{\mathrm{new}} = 247/2$. The dotted line highlights the correlation in the position that the ^{200}At^{1+} and Md^{2+} ions were detected, which led to an $A = 247$ identification for the delivered Md^{2+} ions.

These are listed in Table I. The probability of observing six random correlations when expecting 0.1 is 1.2×10^{-9}, which is determined from a simple Poisson distribution. The expected Q_α for the decay of ^{244}Md is 9.0(2) MeV, which is consistent with the experimental systematics and the local binding energy fits as determined in Ref. [23]. For several of the correlations, the energies of α_1 and α_2 are consistent with what is expected for the decay of ^{244}Md and the subsequent decay of ^{240}Es [24]. To confirm the production of $A = 244$, the BGS focal plane DSSD was retracted and the Md ions were allowed to enter FIONA.

FIONA was calibrated using the $^{198-199}$At^{1+} ions produced in the ^{165}Ho(^{40}Ar, 6-7n) reactions. The mass numbers of the $^{198-199}$At isotopes were identified based on their decay properties [18,19]. The peaks were fit, and the centroid of the ^{198}At peak was found to be in strip 15.64 (11); see Fig. 3 (top). FIONA was scaled from $(A/q)_{\mathrm{cal}} = 198/1$ to $(A/q)_{\mathrm{new}} = 244/2$ for the delivery of the Md^{2+} ions to the FIONA focal plane. Data were collected looking for $A/q = 244/2$ events for ~150 h with the calibration position of the $A/q = 198/1$ ^{198}At^{1+} peak checked approximately every 8 h. Additional calibrations were also performed immediately following each potential $A/q = 244/2$ event to ensure that any potential drifts in the system at the time of the event were detected and taken into account.

TABLE I. The six EVR-α-α events (including one EVR-α-α-α) that were detected at the BGS focal plane and have been assigned to originate with the decay of ^{244}Md due to the successful $A = 244$ mass number determination measured at the FIONA focal plane. These events are listed in order of increasing α_1 energy (E_{α_1}) and are numbered for ease of discussion. The reported error bars are representative of the resolution of the individual strip where each EVR-α-α event was detected. The maximum search time for an EVR-α_1 and for an α_1-α_2 (or α_2-α_3) correlation was 10 and 100 s, respectively.

Evt. no.	E_{α_1} (keV)	EVR-α_1 Δt (s)	E_{α_2} (keV)	α_1-α_2 Δt (s)	E_{α_3} (keV)	α_2-α_3 Δt (s)
1	8178(23)	0.60	7305(23)	27.34	···	···
2	8308(19)	9.18	7996(19)	14.37	···	···
3	8635(18)	0.88	7330(18)	18.95	···	···
4	8653(25)	0.13	8128(25)	1.20	7086(25)	75.97
5	8682(20)	0.31	8203(20)	10.00	···	···
6	8684(20)	1.16	8124(20)	7.65	···	···

In order to distinguish the Md events from the observed background events at the FIONA focal plane, energy, position, and multiplicity criteria were applied to the data. Only events with α energies between 8.35 and 9.00 MeV were considered. This is consistent with the Md α decays observed at the BGS focal plane (see Table I) and the upper limit set by the Q_α value. The trochoidal spectrometer has a vertically narrow exit window that is smaller than the height of the FIONA focal plane DSSD. It was observed during the calibration runs that the $^{198-199}$At^{1+} events were detected only in y strips 8–18. Hence, only potential events detected within that vertical region were considered. The observed events are presented in Fig. 3 (bottom). When FIONA was scaled for $(A/q) = 244/2$, a total of four events were detected in x strips 14 and 15, whose positions correlate with the expected positions of $A/q = 244/2$ ions. Additionally, fission events were looked for, but none were observed.

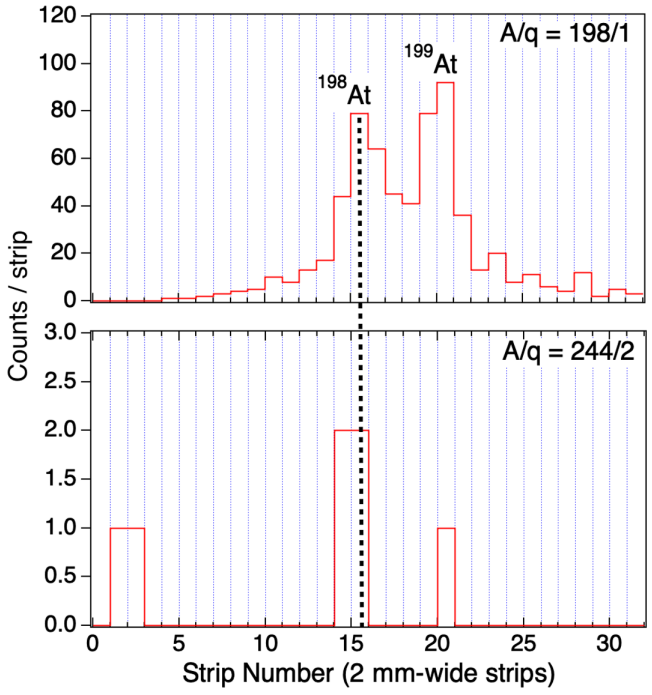

FIG. 3. (Top) Experimental data from an example $^{198-199}$At^{1+} calibration run showing the A/q separation. (Bottom) Location of the detected Md^{2+} ions after FIONA was scaled from $(A/q)_{\text{cal}} = 198/1$ to $(A/q)_{\text{new}} = 244/2$. The dotted line highlights the correlation in the position that the ^{198}At^{1+} and Md^{2+} ions were detected, which led to an $A = 244$ identification for the delivered Md^{2+} ions.

In order to rule out the possibility that the four detected events were random, background was collected for ~25 days following the experiment. For measurements taken at the FIONA focal plane, the background conditions are the same with and without a beam present. These data were analyzed applying the same energy, vertical position, and multiplicity conditions as the in-beam data. Based on this background measurement, we would expect 0.46 random-α events in the three-strip-wide peak corresponding to $A/q = 244/2$ over the six-day beam time. The probability of detecting four random events is on the order of 0.1%. The possibility that the events observed in strips 2, 3, and 20 are random was investigated. There was a 29% probability of detecting one event in strip 20 and a 7% probability of detecting two events in any three-neighboring strips during the duration of the beam time. From this result, $A = 244$ has been assigned to the Md^{2+} ions that were delivered to the FIONA focal plane.

Given the number of events observed at the BGS focal plane and considering that the efficiency of the BGS for this reaction and this size of detector is 32(3)%, we report a cross section of $0.5^{+0.3}_{-0.2}$ nb. A proposed decay scheme for ^{244}Md is presented in Fig. 4 based on the properties of the events listed in Table I. The decay properties of the daughter isotope ^{240}Es have been previously observed in a study of the ^{209}Bi(^{34}S, $3n$)^{240}Es reaction [24]. In Ref. [24], ^{240}Es [$t_{1/2} = 6(2)$ s] was observed to have an ECDF branch to ^{240}Cf [$t_{1/2} = 64(9)$ s] and an α decay to ^{236}Bk ($t_{1/2} = 22^{+13}_{-6}$ s) emitting α particles ranging in energies from 7.97 to 8.19 MeV. The α decays populate ^{236}Bk, which undergoes electron capture (EC) to states in ^{236}Cm [$t_{1/2} = 410(50)$ s]. Due to our constraints on the EVR-α_1 and α_1-α_2 (or α_2-α_3) correlation times of <10 and <100 s, respectively, it is unlikely that any decays attributed to either the ^{240}Es ECDF branch or the ^{236}Bk EC branch would have been observed.

From the events listed in Table I, there is an apparent similarity between events 4, 5, and 6 in the energies of the first- (~8.6 MeV) and second- (~8.1–8.2 MeV) correlated α energies and in their correlation times. The energies and correlation times of the second-correlated α in each of these

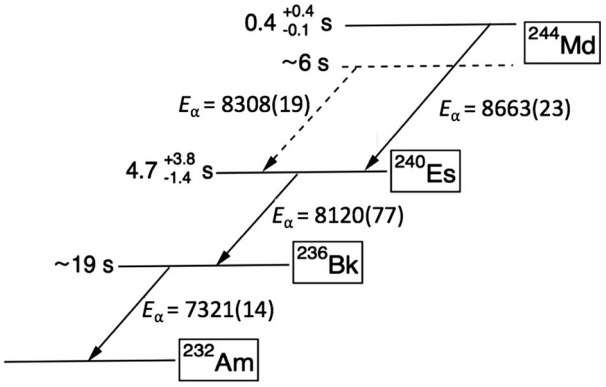

FIG. 4. Partial decay scheme for ^{244}Md, ^{240}Es, and ^{236}Bk created on the basis of the observed events listed in Table I. Tentative assignments are shown as dashed lines. When possible, the presented half-life of the isotope is an average from several observed events. Otherwise, it is shown just as an approximation from a single decay event. The proposed decay scheme is in agreement with what has been observed for ^{240}Es [24]. Energy values are averages of those presented in Table I are given in keV.

events are in agreement with what has been reported for ^{240}Es [24]. Hence, these events are assigned as the α decay of ^{244}Md correlated with the subsequent α decay of ^{240}Es.

The energy of the first α in event 1 of $E_{\alpha 1} = 8178(23)$ keV is similar to what would be expected for a decay from ^{240}Es to ^{236}Bk. The second-correlated α is assigned as the decay of ^{236}Bk to ^{232}Am. We note that there are no previous reports of an α-decay branch from ^{236}Bk [$Q_\alpha = 7780(500)$ keV [25]], only an EC branch to ^{236}Cm [$Q_\alpha = 7067(5)$ keV [25]]. However, as $E_{\alpha 2} = 7305(23)$ keV is greater than Q_α for ^{236}Cm, we have chosen to assign this to a potential decay of ^{236}Bk. Similar α-α correlations were observed (at least in energy; see Fig. 4 in Ref. [24]) but were assigned as random correlations with the decays of the transfer-reaction product ^{213}Rn. No such background was observed in our measurement. Given this, the second α in event 3 is also assigned as the potential α decay of ^{236}Bk, with the first α assigned to the decay of ^{244}Md. In this instance, the decay of ^{240}Es escaped detection. Additionally, there is the possibility that the third-correlated α of event 4 could also be from the decay of ^{236}Bk, but, as $E_{\alpha 3} = 7086(25)$ keV is below Q_α for ^{236}Cm, the decay of either ^{236}Bk or ^{236}Cm is possible.

Finally, the properties of the second α in event 2 fit with an assignment of ^{240}Es, as $E_{\alpha 2} = 7996(19)$ keV is greater than the Q_α values of both ^{236}Cm and ^{236}Bk. However, the energy and correlation time of the first α in this event are different than decays assigned to ^{244}Md in events 3, 4, 5, and 6 [$E_\alpha = 8.66(2)$ MeV and average EVR-$\alpha\Delta t = 0.6^{+0.6}_{-0.2}$ s]. Therefore, the first α is tentatively assigned as the decay of a longer-lived isomeric state in ^{244}Md. Such states have been observed in the neighboring neutron-deficient Md isotopes [22].

The reported half-lives in Fig. 4 are averages of the observed EVR-α_1 or α_1-α_2 correlation times when an assignment was possible. The values of $4.7^{+3.8}_{-1.5}$ and ~19 s for the decays of ^{240}Es and ^{236}Bk, respectively, are in agreement with what has been previously reported [24]. For comparison of the reported $t_{1/2}$ of ^{244}Md, we estimated the expected α-decay half-life for ^{244}Md using the Viola-Seaborg (VS) formula [26], using the parameters in Ref. [27], the Royer formula [28], and the superfluid tunneling model (STM) [29]. We assumed a 100% α-decay branch and estimated $Q_\alpha = 9.0(2)$ MeV. The calculated values were similar for each of the methods: $t_{1/2}(\mathrm{VS}) = 1.0^{+2.7}_{-0.7}$ s, $t_{1/2}(\mathrm{Royer}) = 0.7^{+2.5}_{-0.5}$ s, and $t_{1/2}(\mathrm{STM}) = 1.0^{+2.9}_{-0.8}$ s. These agree well with our experimental value of $t_{1/2} = 0.4^{+0.4}_{-0.1}$ s. This indicates that α decay is likely the dominant decay mode. Though we cannot eliminate the possibility of an EC branch, it is worth noting that the EC of ^{244}Md would result primarily in fission events, either from ECDF (probability expected to be ~50% [30]) or from the spontaneous fission of the ^{244}Fm ground state [31]. No such events were observed at the FIONA focal plane.

In regions where isotopes are produced and studied primarily from fusion-evaporation reactions, the ability to assign decay properties to a specific nucleus via a direct-mass number measurement not only reveals information about that particular nucleus, but it can also serve to clear up potential ambiguities in the entire region due to previous misassignments. In this Letter, we have reported on the identification of the isotope ^{244}Md produced in the ^{209}Bi(^{40}Ar, $5n$) reaction. The mass number assignment $A = 244$ was performed with the FIONA spectrometer, and first decay properties of ^{244}Md are reported. The measured α energies and half-life are consistent with Q_α-value expectations and model calculations. Additionally, this result includes first evidence of the α decay of ^{236}Bk. The direct confirmation of the production of the new isotope ^{244}Md and observation of its decay is the first step toward understanding the properties of this nucleus. Now, further studies can be performed to determine more detailed information on the structure of this nucleus and to search for potential decay modes such as ECDF, which have already been observed for the neighboring odd-odd isotope ^{246}Md [22].

We gratefully acknowledge the operations staff of the 88-inch cyclotron. This work was supported in part by the U.S. Department of Energy, Office of Science, Office of Nuclear Physics under Contract No. DE-AC02-05CH11231 and in part by the Swedish Research Council (VR 2016-3969) and the Knut and Alice Wallenberg foundation (KAW 2015.0021). J. M. G. is supported by a U.S. Department of Energy, Office of

Science, Early Career Award. The work at Lawrence Livermore National Laboratory is performed under the auspices of the U.S. Department of Energy under Contract No. DE-AC52-07NA27344.

*jpore@lbl.gov

[1] A. N. Andreyev, M. Huyse, and P. V. Duppen, Rev. Mod. Phys. **85**, 1541 (2013).
[2] M. Leino, Nucl. Instrum. Methods Phys. Res., Sect. B **204**, 129 (2003).
[3] G. Münzenberg, W. Faust, S. Hofmann, P. Armbruster, K. Güttner, and H. Ewald, Nucl. Instrum. Methods **161**, 65 (1979).
[4] A. V. Yeremin *et al.*, Nucl. Instrum. Methods Phys. Res., Sect. A **274**, 528 (1989).
[5] C. N. Davids and J. D. Larson, Nucl. Instrum. Methods Phys. Res., Sect. B **40–41**, 1224 (1989).
[6] J. M. Gates, EPJ Web Conf. **131**, 08003 (2016).
[7] K. E. Gregorich, Nucl. Instrum. Methods Phys. Res., Sect. A **711**, 47 (2013).
[8] J. M. Gates *et al.*, Phys. Rev. Lett. **121**, 222501 (2018).
[9] J. Khuyagbaatar *et al.* (private communication).
[10] J. L. Pore *et al.*, Phys. Rev. C (to be published).
[11] Z. Q. Xie and C. M. Lyneis, Report No. LBNL-40155, 1997.
[12] Z. W. Chang, J. G. Li, and C. Z. Dong, J. Phys. Chem. A **114**, 13388 (2010).
[13] X. Y. Cao and M. Dolg, Mol. Phys. **101**, 961 (2003).
[14] T. Mariner and W. Bleakney, Rev. Sci. Instrum. **20**, 297 (1949).
[15] G. W. Monk and G. K. Werner, Rev. Sci. Instrum. **20**, 93 (1949).
[16] C. F. Robinson and L. G. Hall, Rev. Sci. Instrum. **27**, 504 (1956).
[17] K. Yano and S. H. Be, Jpn. J. Appl. Phys. **19**, 1019 (1980).
[18] B. Singh, Nucl. Data Sheets **107**, 1531 (2006).
[19] H. Xiaolong and K. Menxiao, Nucl. Data Sheets **121**, 395 (2014).
[20] H. Xiaolong, Nucl. Data Sheets **108**, 1093 (2007).
[21] H. Xiaolong and X. Chunmei, Nucl. Data Sheets **104**, 283 (2005).
[22] S. Antalic *et al.*, Eur. Phys. J. A **43**, 35 (2010).
[23] T. Dong and Z. Ren, Phys. Rev. C **77**, 064310 (2008).
[24] J. Konki *et al.*, Phys. Lett. B **764**, 265 (2017).
[25] M. Wang, G. Audi, F. G. Kondev, W. J. Huang, S. Naimi, and X. Xu, Chin. Phys. C **41**, 030003 (2017).
[26] V. E. Viola and G. T. Seaborg, J. Inorg. Nucl. Chem. **28**, 741 (1966).
[27] A. Parkhomenko and A. Sobiczewski, Acta Phys. Pol. B **36**, 3095 (2005).
[28] G. Royer, Nucl. Phys. **A848**, 279 (2010).
[29] J. Rissanen, R. M. Clark, A. O. Macchiavelli, P. Fallon, C. M. Campbell, and A. Wiens, Phys. Rev. C **90**, 044324 (2014).
[30] J. Khuyagbaatar, Eur. Phys. J. A **55**, 134 (2019).
[31] J. Khuyagbaatar *et al.*, Eur. Phys. J. A **37**, 177 (2008).

Correction: An author name in Ref. [12] was misspelled and has been fixed. The third and fourth affiliations were ordered incorrectly and have been set right.